DALTON
FULL PAPER

Synthesis, crystal structure and magnetic properties of a novel one-dimensional nickel(III) chain complex showing ferromagnetic ordering at low temperature †

Jingli Xie, Xiaoming Ren, You Song,* Yang Zou and Qingjin Meng *

State Key Laboratory of Coordination Chemistry, Coordination Chemistry Institute, Nanjing University, 210093 Nanjing, P.R.China. E-mail: mengqj@netra.nju.edu.cn

Received 22nd February 2002, Accepted 23rd April 2002
First published as an Advance Article on the web 7th June 2002

A novel ferromagnetic complex [BrFBzPy][Ni(mnt)$_2$], where [BrFBzPy]$^+$ = 1-(4′-bromo-2′-fluorobenzyl)pyridinium and mnt^{2-} = maleonitriledithiolate, has been prepared and characterized. In the crystal structure the most prominent feature is that the [Ni(mnt)$_2$]$^-$ anions and [BrFBzPy]$^+$ cations form a well-separated stacking column along the *c*-axis, within which the [Ni(mnt)$_2$]$^-$ anions are uniformly spaced to give a one-dimensional (1-D) chain structure. The magnetic properties of this complex have been investigated in the temperature range 1.8–300 K and its magnetization studies show there exists ferromagnetically coupled interactions within the [Ni(mnt)$_2$]$^-$ anion chain (J = 42.2 cm^{-1}), and antiferromagnetically coupled interactions between [Ni(mnt)$_2$]$^-$ anion chains (J_{eff} = −4.78cm^{-1}). The temperature dependences of the ac susceptibility revealed that this 1-D chain system is ferromagnetically ordered around 2 K and χ_{ac} measurements performed at different magnetic fields and frequencies suggest that there may coexist a degree of spin glass behaviour at low temperature.

Introduction

Recently, 1-D compounds have been attracting widespread attention because they show novel physical properties such as Peierls transitions, spin-Peierls transitions, neutral–ionic transitions, charge density wave (CDW) states, spin density wave (SDW) states, superconductivities, molecular bistabilities, and ability to form molecular magnetic nanowires, *etc*.[1–5] In addition, 1-D compounds have also stimulated theoretical investigations.

One of the most studied classes of 1-D transition metal complexes are the complexes containing [M(mnt)$_2$]$^-$ (mnt^{2-} = maleonitriledithiolate, M = Ni(III), Pd(III) or Pt(III)) ions. In these compounds, the constituent planar molecules [M(mnt)$_2$]$^-$ form columnar stack structures, in which intermolecular d_{z^2} or π orbital interactions result in 1-D electronic nature.[6–9] Usually, the topology and size of the counter cation in the [M(mnt)$_2$]$^-$ complexes may play an important role in controlling the stacking of the anions and cations, which further influence the physical properties of these complexes. We have recently developed a new class of complexes [RBzPy]$^+$[Ni(mnt)$_2$]$^-$ ([RBzPy]$^+$ = benzylpyridinium derivative), and found some significant results.[10] (1) The [RBzPy][Ni(mnt)$_2$] complexes possess crystal structures with well-separated [Ni(mnt)$_2$]$^-$ anions and [RBzPy]$^+$ cations in the solid state, and the [Ni(mnt)$_2$]$^-$ anions form uniformly or alternately spaced 1-D magnetic chains of S = 1/2 along the stacking column in the direction of the anions. (2) The molecular conformation of the [RBzPy]$^+$ cations can be tuned by systematic variation of the substituent groups on the aromatic rings because of their influence on its topology and size. Furthermore, the crystal stacking structure of such complexes could be influenced. Thus the molecular conformation of the [RBzPy]$^+$ cations may have a determinant effect on the crystal stacking structure and could be readily modified by varying the substituent groups on the aromatic rings. (3) This class of 1-D chain complexes has strongly correlated electron systems, and the magnetically coupled interactions in these systems are highly sensitive to any variational intermolecular separation.

In our continuing work with [Ni(mnt)$_2$]$^-$ complexes, we sought to further explore this class of compounds and focus on studying the relationship between the stacking pattern of the anions/cations and the magnetic interactions. Herein, we report the synthesis, structural characterization, and magnetic properties of a 1-D chain [Ni(mnt)$_2$]$^-$ complex showing ferromagnetic ordering at low temperature which may coexist with spin glass behavior. To the best of our knowledge, the uniformly spaced 1-D chain exhibiting ferromagnetism is rare for the [Ni(mnt)$_2$]$^-$ anion.

Experimental

Chemicals and reagents

All manipulations were carried out in air unless otherwise noted. All chemicals and solvents were reagent grade, and were used without further purification. 4-Bromo-2-fluorobenzyl bromide was supplied by Aldrich Chemicals, 1-(4′-bromo-2′-fluorobenzyl)pyridinium bromide ([BrFBzPy]Br), and disodium maleonitriledithiolate (Na$_2$mnt) were synthesized following the published procedures.[11]

Physical measurements

Elemental analyses were performed with a Perkin-Elmer 240 analytical instrument. IR spectra were recorded on a Fourier transform infrared spectrometer (170SX) (KBr pellet).

Magnetic susceptibility data on powder-samples were collected over the temperature range 1.8–300 K using a Quantum Design MPMS-5S superconducting quantum interference device (SQUID) magnetometer, and diamagnetic corrections were made using Pascal's constants. Two different procedures were used: (i) zero-field cooling (ZFC), where the sample was slowly cooled from room temperature down to 1.8 K under zero external field, then a static magnetic field (H) was applied and the magnetization was measured under that field as a function

† Electronic supplementary information (ESI) available: plots of magnetic data. See http://www.rsc.org/suppdata/dt/b2/b201936c/

 DOI: 10.1039/b201936c

Table 1 Summary of crystal and structure refinement data for **2**

Empirical formula	$C_{20}H_{10}BrFN_5NiS_4$
M	606.19
T/K	293(2)
Wavelength/Å	0.71073
Crystal system	Monoclinic
Space group	$P2_1/c$
a/Å	11.989(2)
b/Å	26.363(5)
c/Å	7.4860(15)
β/°	101.63(3)
V/Å^3	2317.5(8)
Z	4
D_c/Mg m^{-3}	1.737
μ/mm^{-1}	2.949
F(000)	1204
Reflections collected	4353
Independent reflections	4022 [R_{int} = 0.0470]
Final R indices [$I > 2\sigma(I)$]	R_1 = 0.0793, wR_2 = 0.2233
R indices (all data)	R_1 = 0.1506, wR_2 = 0.3529

of temperature to get zero-field-cooled magnetization. (ii) Field cooling (FC), where the external static magnetic field was applied to the sample at room temperature and then the sample was cooled down to 2 K in the presence of the field and the field-cooled magnetization M_{FC} data were measured with increasing temperature.

Synthesis of [BrFBzPy]$_2$[Ni(mnt)$_2$] (1)

This compound was prepared by the direct combination of 1 : 2 : 2 mol equiv. of $NiCl_2 \cdot 6H_2O$, Na_2mnt and [BrFBzPy]Br in H_2O. A red precipitate formed which was was filtered off, washed with water and dried under vacuum. Yield: 91% (Found: C, 43.88; H, 2.23; N, 9.69. Calc. for $C_{32}H_{20}Br_2F_2N_6NiS_4$: C, 44.01; H, 2.31; N, 9.62%). IR (cm^{-1}): ν(CN) 2192.9vs, ν(C=C) of mnt^{2-} 1482.1vs.

Synthesis of [BrFBzPy][Ni(mnt)$_2$] (2)

An MeCN solution (10 cm^3) of I_2 (150 mg, 0.59 mmol) was slowly added to a MeCN solution (20 cm^3) of [BrFBzPy]$_2$[Ni(mnt)$_2$] (870 mg, 1.0 mmol), and stirred for 15 min. MeOH (90 cm^3) was then added, and the mixture allowed to stand overnight. The microcrystals which formed were filtered off, washed with MeOH and dried in vacuum. Yield: 83% (Found: C, 39.45; H, 1.62; N, 11.43. Calc. for $C_{20}H_{10}BrFN_5NiS_4$: C, 39.63; H, 1.66; N, 11.55%). IR (cm^{-1}): ν(CN) 2201.8vs, ν(C=C) of mnt^{2-} 1453.5m. Well-formed block single crystals suitable for X-ray analysis were obtained after about a week by dispersing Et_2O into an MeCN solution of **2**.

X-Ray crystallography

Diffraction data for **2** were collected at 293 K on a FR 590 CAD4 diffractometer equipped with graphite-monochromated Mo-Kα radiation. All computations were carried out in a PC-586 computer using the SHELXTL-PC program package.[12] The structure of **2** was solved by direct methods and refined on F^2 by full-matrix least-squares. All non-hydrogen atoms were refined anisotropically. Hydrogen atoms were placed in their calculated positions and refined following the riding model. Crystallographic details for **2** are summarized in Table 1.

CCDC reference number 169414.

See http://www.rsc.org/suppdata/dt/b2/b201936c/ for crystallographic data in CIF or other electronic format.

Results and discussion

Crystal structure

An ORTEP drawing of **2** with non-hydrogen atomic labeling in an asymmetric unit is shown in Fig. 1, selected bond lengths and bond angles are listed in Table 2. For the [Ni(mnt)$_2$]$^-$ anion, the Ni(III) ion is co-ordinated to four sulfur atoms of two mnt^{2-} ligands, and exhibits square-planar coordination geometry. The CN groups of the mnt^{2-} ligand are bent away from the coordinating plane defined by four sulfur atoms. The five-membered nickel-containing rings are slightly puckered, as have been found with other [M(mnt)$_2$]$^{n-}$ structures.[13] The average S–Ni–S bond angle within the five-membered ring is 92.6°, and the average Ni–S bond distance is 2.14 Å, these values are in agreement with those of other [Ni(mnt)$_2$]$^-$ complexes reported.[10] For the ground state conformations of benzylpyridinium derivatives, the studies to date have indicated that the spatial orientation of the aromatic rings depended on both the nature of the electronic and steric properties of the substituent groups.[10,11a] When there is a substituent group on the *ortho*-position of a benzyl, the dihedral angles for the benzene ring and the pyridine ring relative to the C_{Ar}–CH_2–N_{Py} reference plane are far away from 90° owing to steric effects. In the [BrFBzPy]$^+$ cation of **2**, there exists a fluorine atom on the *ortho*-position of the benzyl, however, the cation adopts a conformation in which both the benzene and pyridine rings are nearly perpendicular to the C(15)–C(14)–N(5) reference plane (dihedral angles of 104.1° for the benzene ring, 95.4° for the pyridine ring, respectively). This result may be due to the small size of the fluorine atom and the steric effect can be neglected.

Table 2 Selected bond lengths, bond angles and shorter intermolecular contacts in **2**

Ni(1)–S(1)	2.149(4)	Ni(1)–S(3)	2.143(4)
Ni(1)–S(2)	2.142(4)	Ni(1)–S(4)	2.140(4)
S(1)–Ni(1)–S(2)	92.55(15)	S(2)–Ni(1)–S(3)	84.62(14)
S(3)–Ni(1)–S(4)	92.67(14)	S(1)–Ni(1)–S(4)	90.16(14)
Ni(1) ··· Ni(1)^A	3.96	Br(1) ··· C(15)^A	3.69
Ni(1) ··· Ni(1)^B	3.96	Br(1) ··· C(16)^B	3.67
Ni(1) ··· S(3)^A	3.66	Br(1) ··· C(20)^A	3.80
Ni(1) ··· S(4)^B	3.63	S(2) ··· S(3)^B	3.73

Symmetry codes: A= x, 1.5 − y, −0.5 + z. B= x, 1.5 − y, 0.5 + z.

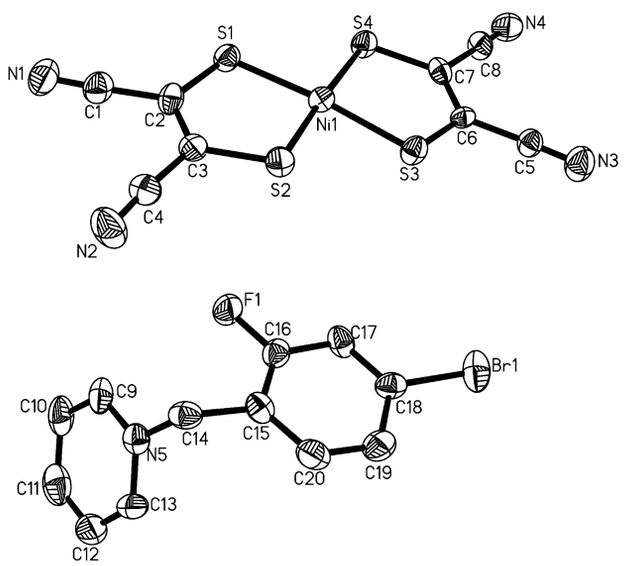

Fig. 1 ORTEP[24] view with non-H atomic numbering scheme for **2**. Ellipsoids are at the 30% probability level.

The most notable structural feature of **2** is that the anions and cations occupy a stacking structure within well-separated columns along the c-axis (Fig. 2); some shorter intermolecular contacts are shown in Table 2. Within an anion column, the [Ni(mnt)$_2$]$^-$ anions form a 1-D uniformly spaced chain, and the slipped nickel-over-sulfur configuration of the [Ni(mnt)$_2$]$^-$ anions is displayed in Fig. 3. The nearest S ··· S, S ··· Ni and

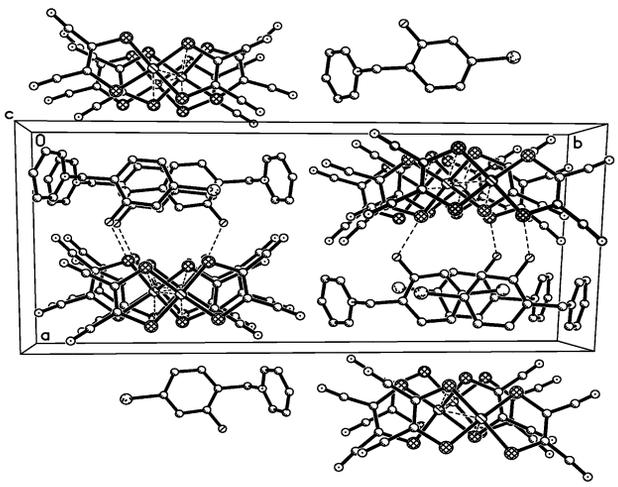

Fig. 2 The packing diagram of a unit cell of **2**.

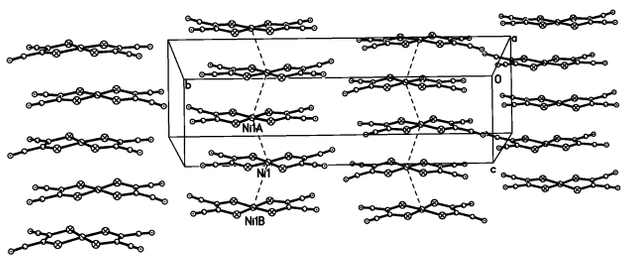

Fig. 3 The side view of the 1-D anion chain in **2** with the cell outline (symmetry codes: A = x, 1.5 − y, −0.5 + z; B = x, 1.5 − y, 0.5 + z).

Ni ··· Ni distances are of 3.73, 3.63 and 3.96 Å within the $[Ni(mnt)_2]^-$ anion chain, respectively. The distances are larger than the sum of van der Waals radii of the corresponding atoms. The closest Ni ··· Ni separation between anion chains is 11.89 Å, which is significantly longer than the Ni ··· Ni separation within a chain. Obviously, there are intermolecular interactions between neighboring $[Ni(mnt)_2]^-$ anions due to the shorter intermolecular separations. Originally, the $[Ni(mnt)_2]^-$ anion chain was considered to be a one-dimensional magnetic chain with negligible interchain interactions. On condition that the Ni ··· Ni separation between the anion chains is of the same magnitude as the distance of the Ni ··· Ni separation within an anion chain and interchain interactions are not neglected, the 1-D character in this complex is damped.[14] For **2**, moreover, the magnetic interaction between two anion columns separated by a sizable diamagnetic cation column is generally weak. The $[BrFBzPy]^+$ cations orient themselves in the solid state. The benzene rings of neighboring benzyl moieties are parallel to each other. The Br atoms overlap with the adjacent benzene rings, with shorter intermolecular separations occuring between Br(1) and C(15)^A, Br(1) and C(16)^B, Br(1) and C(20)^A (Table 2). The cations thus form a 1-D chain through Br–π interactions between the Br atoms and adjacent benzene rings. This phenomenon has also been found in some halogenobenzene derivatives in the solid state, and is due to p–π interactions between the halogen atoms and the benzene rings.[15] Therefore, from the point of view of the structure analysis, **2** is an ideal 1-D magnetic chain system.

Magnetic properties

The magnetic properties of **2** have been investigated in the temperature range 1.8–300 K, and the χ_mT *versus* T plot is displayed in Fig. 4, in which χ_m is the molar magnetic susceptibility. The value of χ_mT at 300 K is estimated at 0.412 emu K mol^{-1}, and is slightly larger than that of a spin-only S = 1/2 spin per formula unit. The χ_mT values increase as the temperature decreases and reaches a maximum at 3.7 K (χ_mT = 2.55 emu K mol^{-1}). The results described above demonstrate the presence of ferromagnetic exchange interactions between the localized spins (neighboring Ni(III) ions). When the temperature is below 3.7 K, the χ_mT values decrease and drop to 1.58 emu K mol^{-1} at 1.82 K suggestive of the presence of a weak intermolecular antiferromagnetic interaction. In the temperature range 5–300 K, an estimation was made by fitting χ_m data to the Baker equation[16] (expression (1) applicable for chain of S = 1/2 spin) derived from a high-temperature series expansion. A fit of the data to eqn. (1) gives g = 2.09, J = 42.2 cm^{-1}, TIP = 7.5 × 10^{-5} emu with a final agreement factor R = 2.5 × 10^{-3} [$R = \Sigma(\chi_mT^{obs} - \chi_mT^{calc})^2/\Sigma(\chi_mT^{obs})^2$].

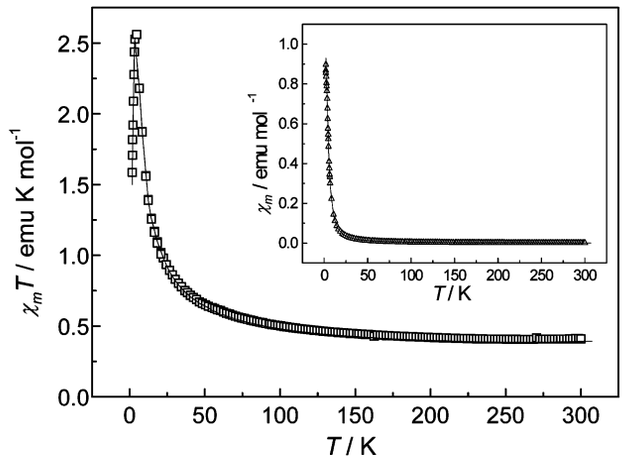

Fig. 4 Plots of χ_mT (□) and χ_m (Δ) of **2** measured at 5 kOe. The solid line represents the best fit.

$$\chi_m = \frac{Ng^2\beta^2}{4kT}\left[\frac{C}{D}\right]^{2/3}$$
$$C = 1.0 + 5.7979916y + 16.902653y^2 + 29.376885y^3 + 29.832959y^4 + 14.036918y^5$$
$$D = 1.0 + 2.7979916y + 7.0086780y^2 + 8.653644y^3 + 4.5743114y^4 \quad (1)$$
$$y = J/2kT$$

As mentioned above, there may exist an interchain antiferromagnetic coupling and it should be further considered. Thus, a two-dimensional model involving a "chain of chains"[17] with large coupling within the chains and weak coupling between the chains was attempted to fit the data from 300 to 3 K. In this model, at a given temperature, an effective total spin associated with each chain in the structure, S_{eff}, can be calculated as shown in eqn. (2), where χ_{FC} is the susceptibility calculated for the ferromagnetic chain from eqn. (1).

$$S_{eff}(T) = -\frac{1}{2} + \frac{1}{2}\sqrt{1 + 8\chi_{FC}T} \quad (2)$$

Below 5 K, the $\chi_{FC}T$ values are quite large ($\chi_{FC}T$ > 2.3) so that the S_{eff} value derived from eqn. (2) is large enough (S_{eff} > 1.7) to be treated as a classic spin.[17a] In this case, it should be acceptable to use the classic spin model (eqn. (3)) derived by Fisher[18] to treat the magnetic susceptibility (χ_{2D}) of this "chain of chains" model.[17]

From eqn. (3), the full fitting parameters are as follows: g = 2.09, J = 42.2 cm^{-1}, g_{eff} = 2.0 (fixed), J_{eff} = −4.78 cm^{-1}. The plot of the experimental data for **2** and the theoretical line

$$\chi_m = \frac{Ng^2\beta^2}{3kT}S_{eff}(S_{eff}+1)\frac{(1+u)}{(1-u)} \quad (3)$$
$$u = \coth[J_{eff}S_{eff}(S_{eff}+1)/kT] - kT/S_{eff}(S_{eff}+1)$$

(solid line) are illustrated in Fig. 4. The fitting results indicated that there exist ferromagnetically coupled interactions within the $[Ni(mnt)_2]^-$ anion chain, and antiferromagnetically coupled interactions between $[Ni(mnt)_2]^-$ anion chains.

From the above results it can be seen that a short-range ferromagnetic correlation is present in this 1-D chain system, and it may develop into a long range ordering state below 2 K. The field-cooled (FC) magnetizations at different dc field and zero-field-cooled (ZFC) magnetization measured between 1.8 and 30 K, along with remnant magnetization data, are shown in Fig. 5. The FCM curve obtained upon cooling the sample with

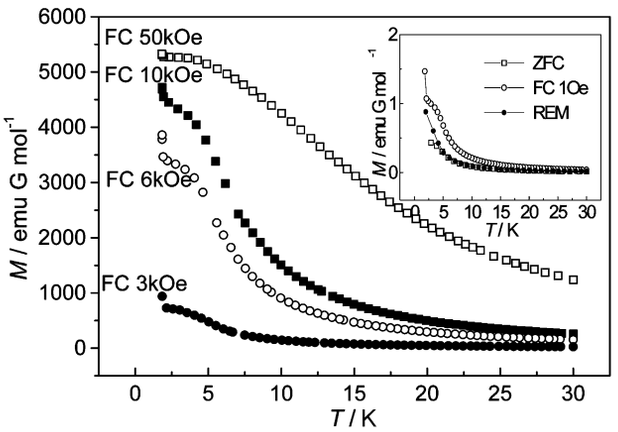

Fig. 5 Field-cooled, zero-field-cooled and remnant magnetization (M/T) data for **2**.

an applied field of 1 Oe displays a gradual change from 30 to 3 K indicating the presence of a short-range magnetic correlation, but a sharp rise around 2 K, demonstrating a long range order transition. At low temperatures, the FC curve lies above the ZFC ones as a result of increased alignment of these ferromagnetic entities on cooling in the presence of a magnetic field (*cf.* the inset of Fig. 5). At different measured fields (3–50 kOe), similar changes between 30 and 1.8 K were observed in the FCM curves.

To confirm the appearance of magnetic ordering and to determine the critical temperature precisely, ac susceptibility measurements were performed. Typically, in a magnet containing net magnetic moments in the ordered state (ferromagnet, ferrimagnet, or canted antiferromagnet, for example), these measurements show a maximum in the in-phase signal (χ') near T_c and the out-of-phase signal (χ'') starts to appear at temperatures just below T_c. In **2**, χ' shows a maximum around 2 K indicating that the magnetic ordering may occur near this temperature, and the nonzero χ'' was also observed below 2 K (Fig. 6). That the nature of the magnetic transition in this 1-D chain system corresponds to the ferromagnetic interaction is demonstrated further by the field dependence of the isothermal magnetization performed at 2, 5 and 10 K, respectively (Fig. S1a, ESI).† The magnetization at 2 K increases very rapidly at low fields, and reaches a saturation value of *ca.* 5400 emu G mol^{-1} at 50 kOe, which agrees well with the theoretical saturation value of a $S = 1/2$, $g = 2$ system (when Ni(III) is in a low spin state). The rapid rise and approach to saturation in the $M(H)$ data is typical for long range ferromagnetic coupling at low temperature (2 K). On the contrary, the magnetization at 5 and 10 K increases slowly as the magnetic field increases. The magnetic data (*M versus H*) at 2 K were fitted by the following equation:

$$M = NgJ\mu_B B_J(y) \quad (4)$$

where $B_J(y) = (2J + 1)(2J)^{-1}\coth[\{(2J + 1)(2J)^{-1}\}y] - (2J)^{-1}\coth[y(2J)^{-1}]$ is the Brillouin function, $y = gJ\mu_B H/k_B T$ and

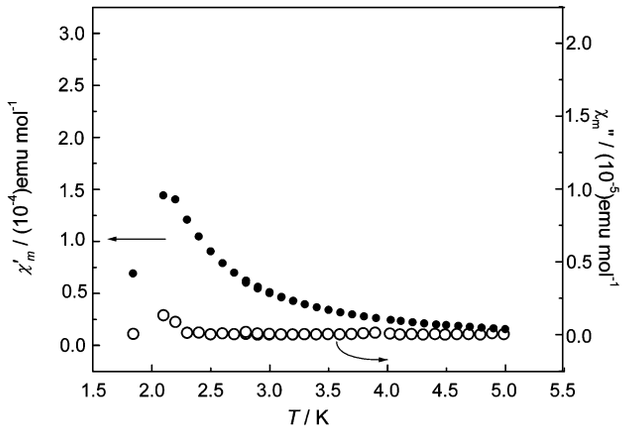

Fig. 6 Temperature dependence of the ac susceptibility obtained at zero external magnetic field.

all parameters have their usual meaning. The best fit for it leads to $g = 2.11$ and this value is close to the result mentioned above. Cycling the applied field between +50 kOe and −50 kOe at 2 K, only a very small observable hysteresis loop, characteristic of ferromagnetic behavior, arises (Fig. S1b, ESI).†

To gain a deeper insight into the magnetic properties of **2**, χ_{ac} measurements with varying external applied magnetic fields (300–3 kOe) (Fig. S2, ESI)† and frequencies (0.1–5 Hz) (Fig. S3, ESI)† are performed. In Fig. S2a† it is shown that the real part of χ_{ac} (χ') exhibits a maximum at 2.2 K when the magnetic field is 300 Oe, in agreement with the above results; upon increasing the field, the maxima get flattened and shift towards higher temperatures. Similar phenomena are observed in the χ'' magnetic susceptibilities (Fig. S2b, ESI).† This phenomena possesses characteristics akin to the literature on spin glass behavior which have been reported for the oxide Ba_2ScCoO_5 and $Ni(C_2H_8N_2)_2NO_2(ClO_4)$ abbreviated as NENP spin-glass systems.[19] However, as the frequency increased from 0.1 to 5 Hz, there was no obvious frequency dependence of χ' and χ'' (Fig. S3, ESI).† Additionally, it is notable that for higher frequencies (7 Hz and above), the measurements become very noisy similar to previously reported phenomena.[20] At this stage, we infer that there may coexist spin glass behavior. This is probably caused by the competition between the ferromagnetic and antiferromagnetic states.

Generally, the origin of the ferromagnetically coupled interaction can be explained in terms of two factors for neighboring metal centers,[6,21] that is, either orbital symmetry or spin polarization effects. From the crystal structure analysis of **2**, there is only a $[Ni(mnt)_2]^-$ ion in an asymmetric unit, neighboring $[Ni(mnt)_2]^-$ anions are related by symmetry operations. So four anions in a cell have the same symmetry. Based on the magnetic orbital model,[14,22] the orbitals describing the unpaired electron (the so called magnetic orbitals) and centered on each Ni(III) ion have the same symmetry, hence, spin delocalization between Ni(III) ions should cause weak but non-negligible antiferromagnetic interactions due to its considerably small orbital overlap with the SOMOs of the $[Ni(mnt)_2]^-$ ions in spite of the presence of short intermolecular atomic contacts (see Table 2). In the light of the discussions above, the observed larger ferromagnetic interaction should occur as a result of spin polarization effects (McConnell's theory).[23] The spin polarization effect gives rise to ferromagnetic interactions, that is to say, noncompensating regions of positive and negative spin densities, here distributed over the atomic sites of the $[Ni(mnt)_2]^-$ complex, and the assembling of the units in an 'up–down' fashion as depicted in Fig. 7 (namely through this antiferromagnetic interaction between the large positive spin density of a unit and the small negative spin density of the adjacent unit, the ultimate result is the ferromagnetic interaction between the large positive spin densities on the Ni atoms of neighboring $[Ni(mnt)_2]^-$).[1,6]

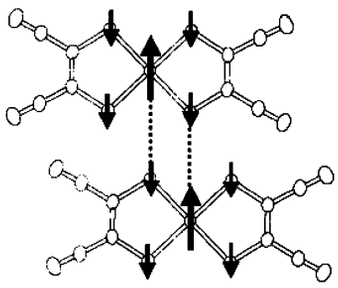

Fig. 7 Schematic representation of spin density in $[Ni(mnt)_2]^-$. The dotted line shows the 'local' antiferromagnetic interactions.

Fig. 3 shows a slipped Ni-over-S configuration within the $[Ni(mnt)_2]^-$ anion chain, therefore, based on the opinions of Nishijo *et al.*,[6] the origin of the ferromagnetically coupled interactions in **2** arises from the spin polarization effect between large positive spin densities on the Ni(III) ions and small negative spin densities on the S atoms of adjacent $[Ni(mnt)_2]^-$ ions.

Conclusions

In this work, we have synthesised a novel 1-D ferromagnetic chain complex [BrFBzPy][Ni(mnt)$_2$]. Its crystal structure revealed that the $[Ni(mnt)_2]^-$ anions form a uniformly spaced 1-D chain. The magnetic properties of this complex have been investigated in the temperature range 1.8–300 K, and the corresponding results show that there exists ferromagnetically coupled interactions within the $[Ni(mnt)_2]^-$ anion chain, and antiferromagnetically coupled interactions between $[Ni(mnt)_2]^-$ anion chains. In the lowest temperature region, the $\chi_m T$ values decrease with decreasing temperature and this may arise from non-compensated antiferromagnetism between anion chains (*cf.* Fig. 7). This 1-D chain system is ferromagnetically ordered and may coexist with spin glass behaviour around 2 K. In the current studies, we selected the $[Ni(mnt)_2]^-$ anion and derivative of benzylpyrinium as architectural blocks for a low-dimensional molecular solid. The results obtained here will be of use in establishing a design strategy for tailoring one-dimensional (1-D) magnetic structures and it might be useful for exploring other molecule systems. In addition, the low-dimensional systems containing the planar-square $[M(mnt)_2]^-$ ion provide good examples for researching the aspects of novel physical properties.

Acknowledgements

The authors gratefully acknowledge the helpful suggestions of the referees. This project was supported by the National Natural Science Foundation, the State Education Commission of China and the State Key Laboratory of Structural Chemistry.

References

1 A. T. Coomber, D. Beljonne, R. H. Friend, J. L. Brédas, A. Charlton, N. Robertson, A. E. Underhill, M. Kurmoo and P. Day, *Nature (London)*, 1996, **380**, 144.
2 T. Manabe, T. Kawashima, T. Ishii, H. Matsuzaka, M. Yamashita, T. Mitani and H. Okamoto, *Synth. Met.*, 2001, **116**, 415.
3 J. H. Wei, J. Q. Zhao, D. S. Liu, S. J. Xie, L. M. Mei and J. Hong, *Synth. Met.*, 2001, **122**, 305.
4 W. Fujita and K. Awaga, *Science*, 1999, **286**, 261.
5 A. Caneschi, D. Gatteschi, N. Lalioti, C. Sangregorio, R. Sessoli, G. Venturi, A. Vingingni, A. Rettori, M. G. Pini and M. A. Novak, *Angew. Chem., Int. Ed.*, 2001, **40**, 1760.
6 J. Nishijo, E. Ogura, J. Yamaura, A. Miyazaki, T. Enoki, T. Takano, Y. Kuwatani and M. Iyoda, *Solid State Commun.*, 2000, **116**, 661.
7 A. E. Pullen, C. Faulmann, K. I. Pokhodnya, P. Cassoux and M. Tokumoto, *Inorg. Chem.*, 1998, **37**, 6714.
8 M. L. Allan, A. T. I. R. Coomber, J. Marsden, H. F. Martens, R. H. Friend, A. Charlton and A. E. Underhill, *Synth. Met.*, 1993, **55–57**, 3317.
9 A. Kobayashi, Y. Sasaki, H. Kobayashi, A. E. Underhill and M. M. Ahmad, *J. Chem. Soc., Dalton Trans.*, 1982, 390.
10 (*a*) X. M. Ren, C. S. Lu, Y. J. Liu, H. Z. Zhu, H. F. Li, C. J. Hu and Q. J. Meng, *Transition Met. Chem.*, 2001, **26**, 136; (*b*) X. M. Ren, H. F. Li, P. H. Wu and Q. J. Meng, *Acta Crystallogr., Sect. C*, 2001, **57**, 1022; (*c*) X. H. Zhu, X. Z. You, X. M. Ren, W. L. Tan, W. Dai, S. S. S. Raj and H. K. Fun, *Chem. Lett.*, 2000, 472.
11 (*a*) S. B. Bulgarevich, D. V. Bren, D. Y. Movshovic, P. Finocchiaro and S. Failla, *THEOCHEM*, 1994, **317**, 147; (*b*) A. Davison and H. R. Holm, *Inorg. Synth.*, 1967, **10**, 8.
12 G. M. Sheldrick, SHELXTL, Structure Determination Software Programs, Version 5.10, Siemens Analytical X-Ray Instruments, Madison, WI, 1997.
13 K. W. Plumlee, B. M. Hoffman and J. A. Ibers, *J. Chem. Phys.*, 1975, **63**, 1926.
14 M. Verdaguer, *Polyhedron*, 2001, **20**, 1115.
15 (*a*) M. R. Sundberg, *Inorg. Chim. Acta*, 1998, **267**, 249; (*b*) R. Sillanpää, J. Jokela and M. R. Sundberg, *Inorg. Chim. Acta*, 1997, **258**, 221; (*c*) M. R. Sundberg and R. Sillanpää, *Acta Chem. Scand.*, 1992, **46**, 34.
16 (*a*) G. A. Baker, G. S. Rushbrooke and H. E. Gilbert, *Phys. Rev.*, 1964, **135**, A1272; (*b*) L. Deakin, A. M. Arif and J. S. Miller, *Inorg. Chem.*, 1999, **38**, 5072.
17 (*a*) L. K. Thompson, S. S. Tandon, F. Lloret, J. Cano and M. Julve, *Inorg. Chem.*, 1997, **36**, 3301; (*b*) A. Caneschi, D. Gatteschi, M. C. Melandri, P. Rey and R. Sessoli, *Inorg. Chem.*, 1990, **29**, 4228; (*c*) F. Lloret, R. Ruiz, M. Julve, J. Faus, Y. Journaux, L. Castro and M. Verdaguer, *Chem. Mater.*, 1992, **4**, 1150.
18 M. E. Fisher, *Am. J. Phys.*, 1964, **32**, 343.
19 (*a*) I. J. Ortega, R. S. Puche, J. R. de Paz and J. L. Martínez, *J. Mater. Chem.*, 1999, **9**, 525; (*b*) M. Hagiwara, K. Katsumata, S. Sasaki, N. Narita, I. Yamada and T. Yosida, *J. Appl. Phys.*, 1996, **79**, 6167.
20 P. Rabu, P. Janvier and B. Bujoli, *J. Mater. Chem.*, 1999, **9**, 1323.
21 I. Fernández, R. Ruiz, J. Faus, M. Julve, F. Lloret, J. Cano, X. Ottenwaelder, Y. Journaux and M. C. Muñoz, *Angew. Chem., Int. Ed.*, 2001, **40**, 3039.
22 (*a*) S. Ohkoshi and K. Hashimoto, *Chem. Phys. Lett.*, 1999, **314**, 210; (*b*) O. Kahn, *Inorg. Chim. Acta*, 1982, **62**, 3; (*c*) O. Kahn and B. Briat, *J. Chem. Soc., Faraday Trans. 2.*, 1976, **2**, 268; O. Kahn and B. Briat, *J. Chem. Soc., Faraday Trans. 2*, 1976, **8**, 1441.
23 H. M. McConnell, *J. Chem. Phys.*, 1963, **39**, 1910.
24 C. K. Johnson, ORTEP, Report ORNL-5138, Oak Ridge National Laboratory, Oak Ridge, TN, 1976.